

Universidade Federal de Alagoas  
Instituto de Computação  
Laboratório de Computação Científica e Análise Numérica

## **Research report**

Student: Danilo Fernandes Costa

Professor: Alejandro Frery

September  
2019

# 1 Introduction

In this report, some results of the analysis of samples referring to plantation regions observed over time are shown. The first observation was made on 16 May 2016, which was followed by four others with a time interval of 25 days between adjacent observations. Those regions consist of three soybeans crops, three wheat, two oats and two canola and are shown in the figures 2(a) to 2(e). Those samples were obtained using the classification of the regions given in the figure 1.

The results consist of the graphic adjusting of the beta distribution to the histograms of the distances of the samples to the trihedral and random volume scatterers. In addition, the Kolmogorov-Smirnov good-of-fit test was performed to validate the hypothesis of the adjust. The choice of these scatterers is because they were more sensitive to vegetation variation in the analyzed regions, which can be verified in the figures 3(a) and 3(b) that contain respectively the pixel proportions in the sample that is more similar to trihedral and the random volume as a function of time.



Figura 1: Classification of the regions on the PolSAR image

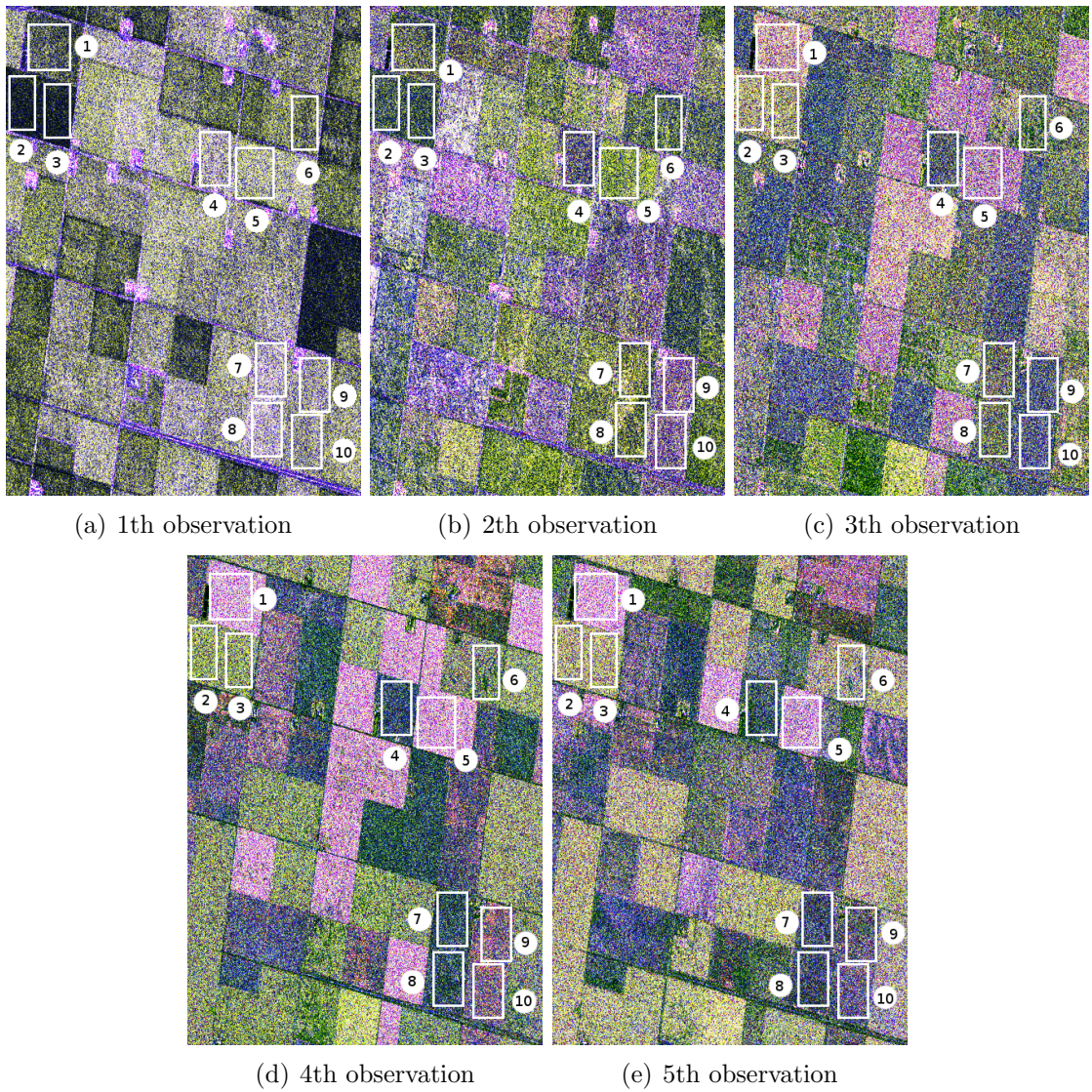


Figura 2: Samples analysed over time in where 1 to 10 corresponding respectively to Canola 43, Soybeans 231, Soybeans 232, Wheat 225, Canola 224, Soybeans 101, Oats 102, Oats 103, Wheat 105 and Wheat 104

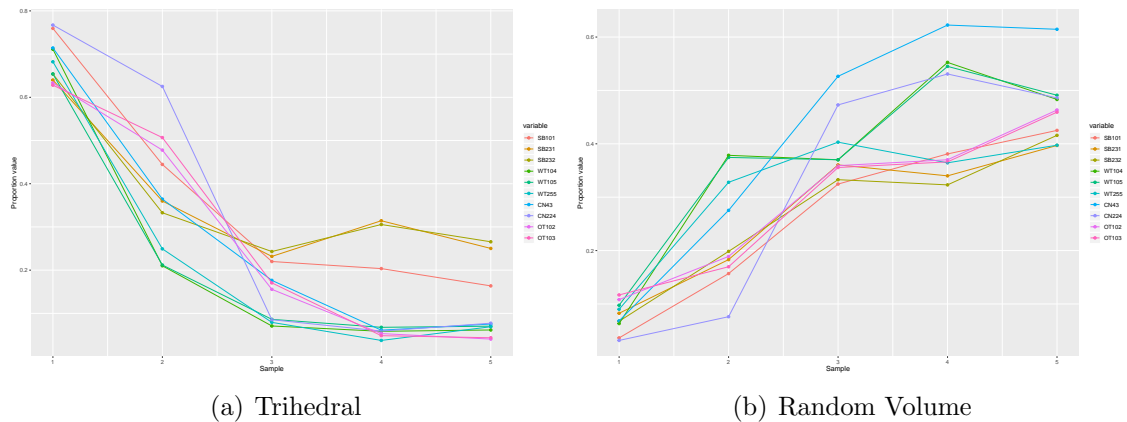


Figura 3: Pixel proportions on the analysed regions more similar to trihedral and random volume as function of time, where SB, WT, CN and OT indicate respectively Soybeans, Wheat, Canola and Oats

## 2 Adjust the histograms to the Beta Distribution

The figures 4 to 23 contain the histograms of the Geodesic Distances between the scatterer (random or trihedral volume) and the pixels of the sample most similar to this scatterer. The number of those pixels are in the table 1 which TR and RV indicates respectively trihedral and random volume. In addition, the histograms are graphically adjusted by the Beta Distribution, whose parameters were estimated from the distances analyzed.

Those adjusts was verified by Komolgorov-Smirnov good-of-fit test whose obtained  $p$ -values are in the table 2. In this table, the biggest and least  $p$ -values are in bold.

Tabela 1: Number of pixels more similar to trihedral and random volume

	First observation		Second observation		Third observation		Fourth observation		Fifth observation	
	TR	RV	TR	RV	TR	RV	TR	RV	TR	RV
<b>SB 101</b>	1481	71	867	306	429	633	397	743	319	829
<b>SB 231</b>	1285	148	656	381	449	706	615	649	508	775
<b>SB 232</b>	1275	132	649	387	474	649	596	630	518	811
<b>WT 104</b>	1618	144	478	861	161	842	133	1257	140	1099
<b>WT 105</b>	1488	222	482	852	196	842	154	1240	160	1117
<b>WT 255</b>	1552	205	567	746	180	917	85	829	157	904
<b>CN 43</b>	1964	155	1002	625	485	1195	168	1413	207	1395
<b>CN 224</b>	2106	87	1716	209	234	1298	162	1457	212	1334
<b>OT 102</b>	1441	246	1087	430	354	817	121	842	92	1054
<b>OT 103</b>	1429	266	1153	386	388	806	110	833	99	1045

Tabela 2:  $p$ -values of the Kolmogorov-Smirnov goodness-of-fit test of the distances to trihedral an random volume

	First observation		Second observation		Third observation		Fourth observation		Fifth observation	
	TR	RV	TR	RV	TR	RV	TR	RV	TR	RV
<b>SB 101</b>	0.065	0.517	0.947	0.758	<b>0.059</b>	0.495	0.452	0.109	0.401	0.144
<b>SB 231</b>	0.775	0.242	0.573	0.166	0.314	0.275	0.239	0.114	0.416	0.070
<b>SB 232</b>	0.244	0.340	0.968	0.328	0.713	0.070	0.422	0.357	0.163	0.630
<b>WT 104</b>	0.178	0.715	0.421	0.094	0.514	0.779	0.062	0.369	0.602	0.919
<b>WT 105</b>	0.231	0.090	0.069	0.139	0.557	0.613	0.108	0.195	0.192	0.252
<b>WT 255</b>	0.235	0.513	0.270	0.375	0.628	0.279	0.653	0.069	0.437	<b>0.993</b>
<b>CN 43</b>	0.238	0.406	0.217	0.202	0.930	0.318	0.623	0.732	0.262	0.747
<b>CN 224</b>	0.184	0.116	0.128	0.333	0.298	0.714	0.813	0.409	0.305	0.391
<b>OT 102</b>	0.289	0.191	0.243	0.532	0.384	0.212	0.710	0.370	0.928	0.396
<b>OT 103</b>	0.096	0.139	0.139	0.186	0.265	0.079	0.936	0.079	0.989	0.489

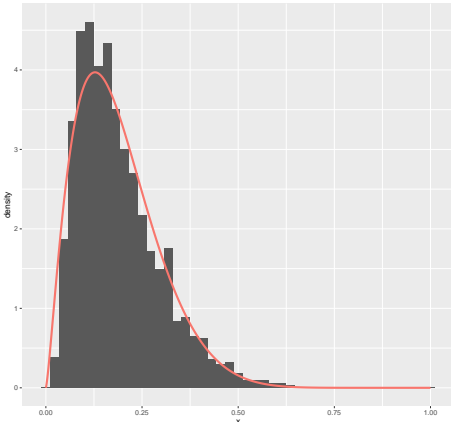
### **3 Parameters evaluation**

When observing the region referring to Soybeans 231 along its samples in the figure 2, which is indexed by 2, it can be assumed that there was a gradual increase in the degree of vegetation of this region.

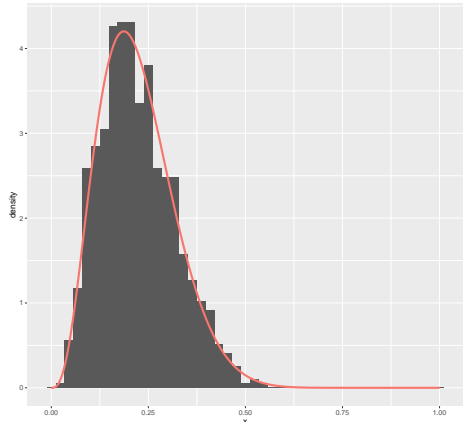
In order to relate this to the variation of the information contained in the distances of its data to the trihedral, the graph of the figure 24 was produced. For each observation, it contains a boxplot of the means of the distances between trihedral and the subregions generated by dividing region 2 into 45 subregions with 7x6 dimensions. In addition, all boxplots were connected by the mean of their means.

### **4 Conclusions**

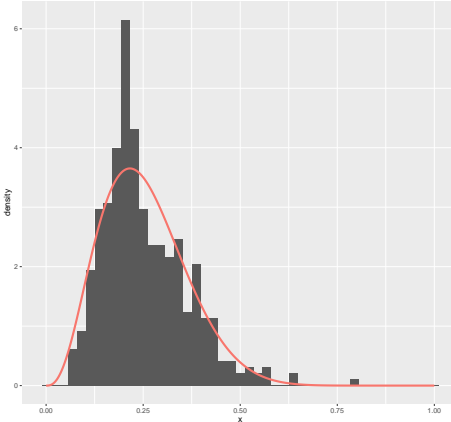
It can be concluded from the  $p$ -values table that the Beta distribution adjusts the distances of PolSAR data of the analyzed cultures to trihedral and random volume at the significance level of 0.05.



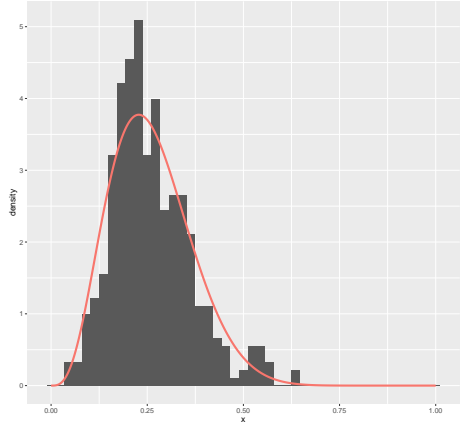
(a) 1th observation



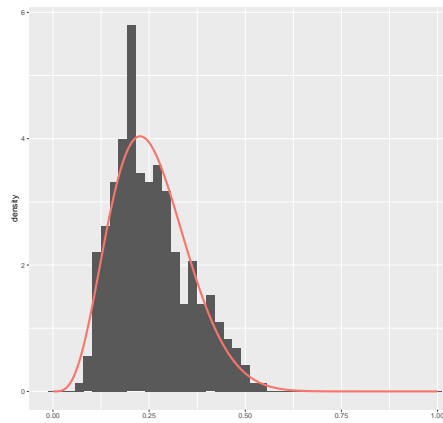
(b) 2th observation



(c) 3th observation



(d) 4th observation



(e) 5th observation

Figura 4: Histograms of the Geodesic Distances between trihedral and the pixels of the sample extracted from Soybeans 101 most similar to trihedral

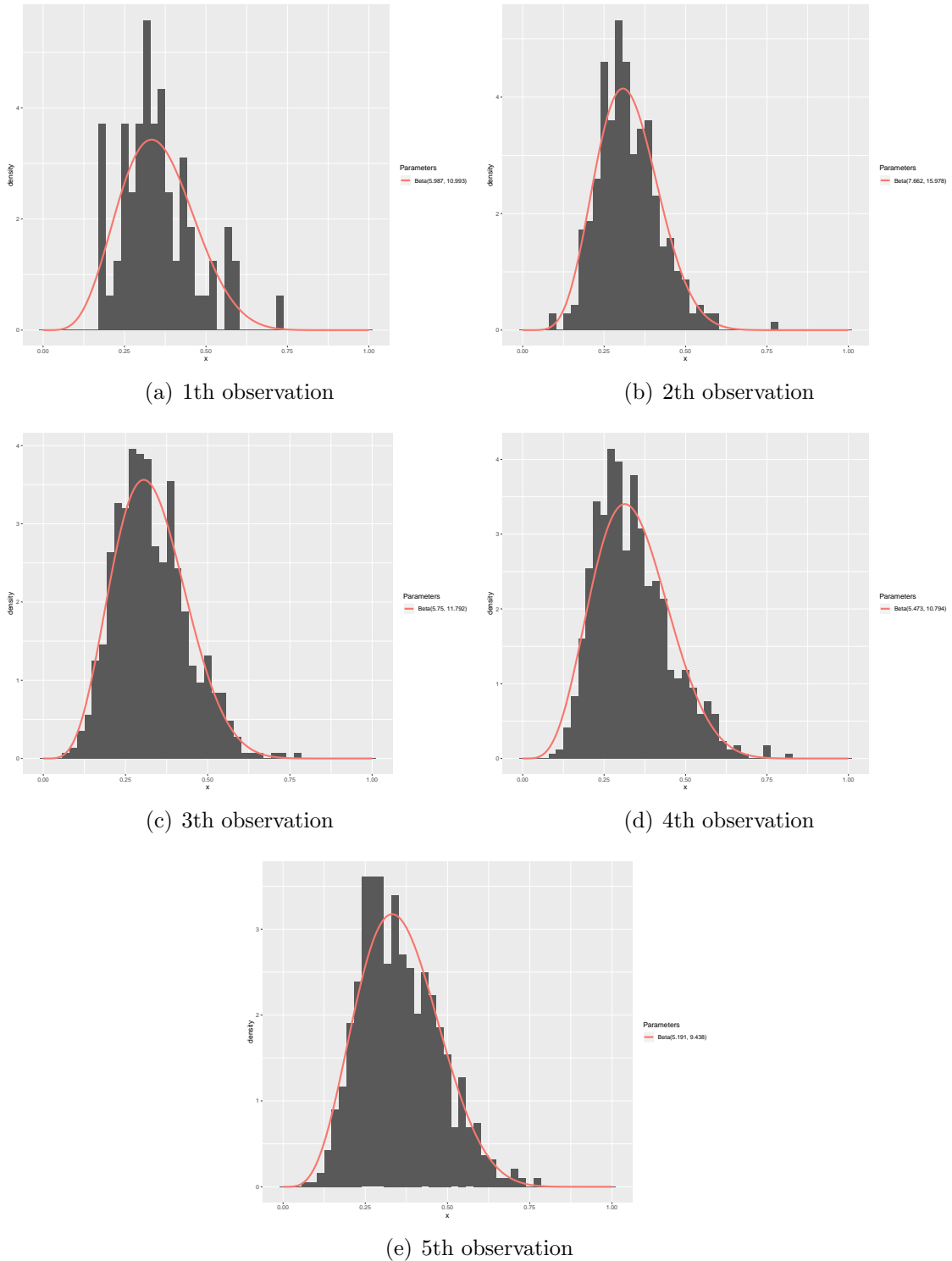


Figura 5: Histograms of the Geodesic Distances between random volume and the pixels of the sample extracted from Soybeans 101 most similar to random volume

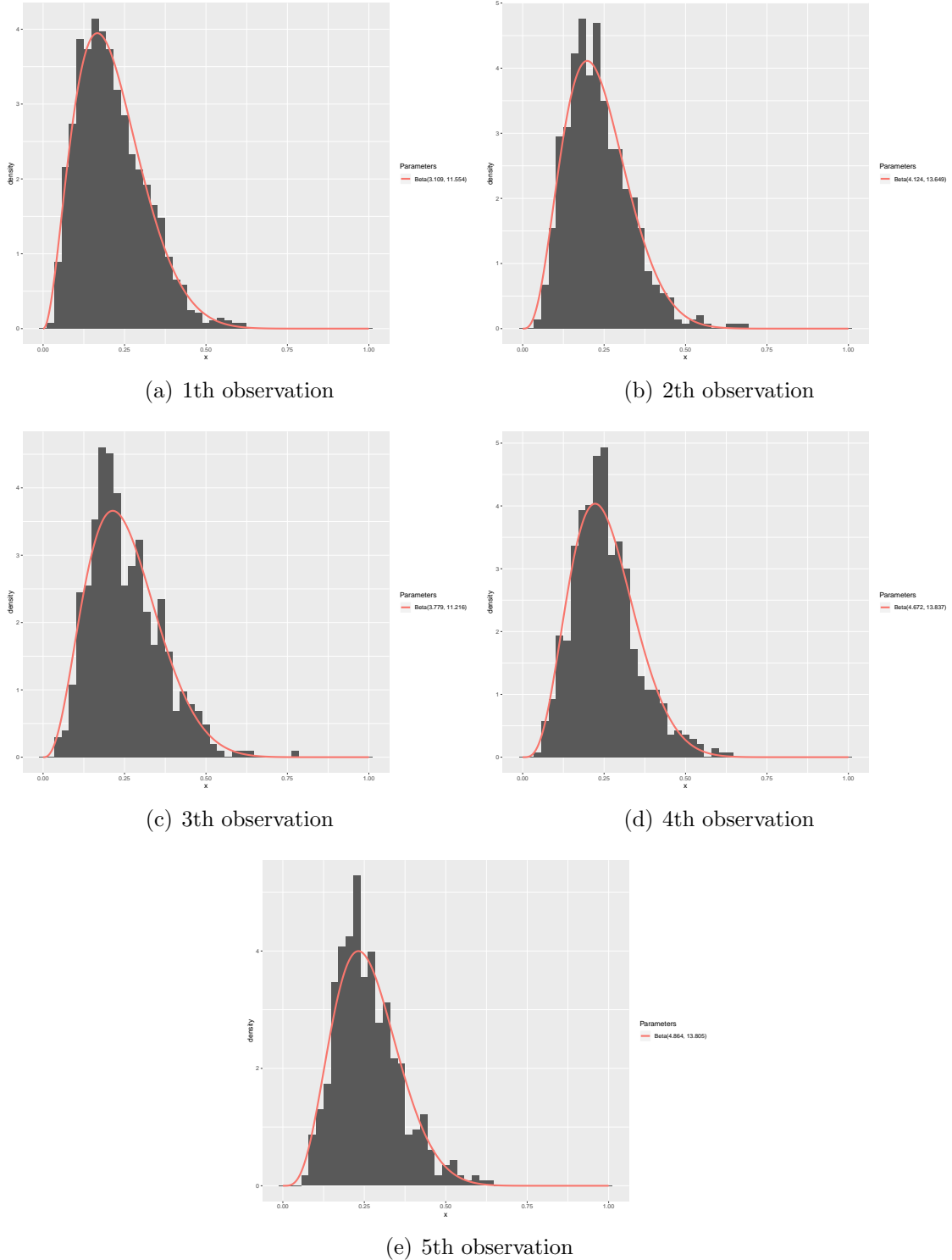


Figura 6: Histograms of the Geodesic Distances between trihedral and the pixels of the sample extracted from Soybeans 231 most similar to trihedral

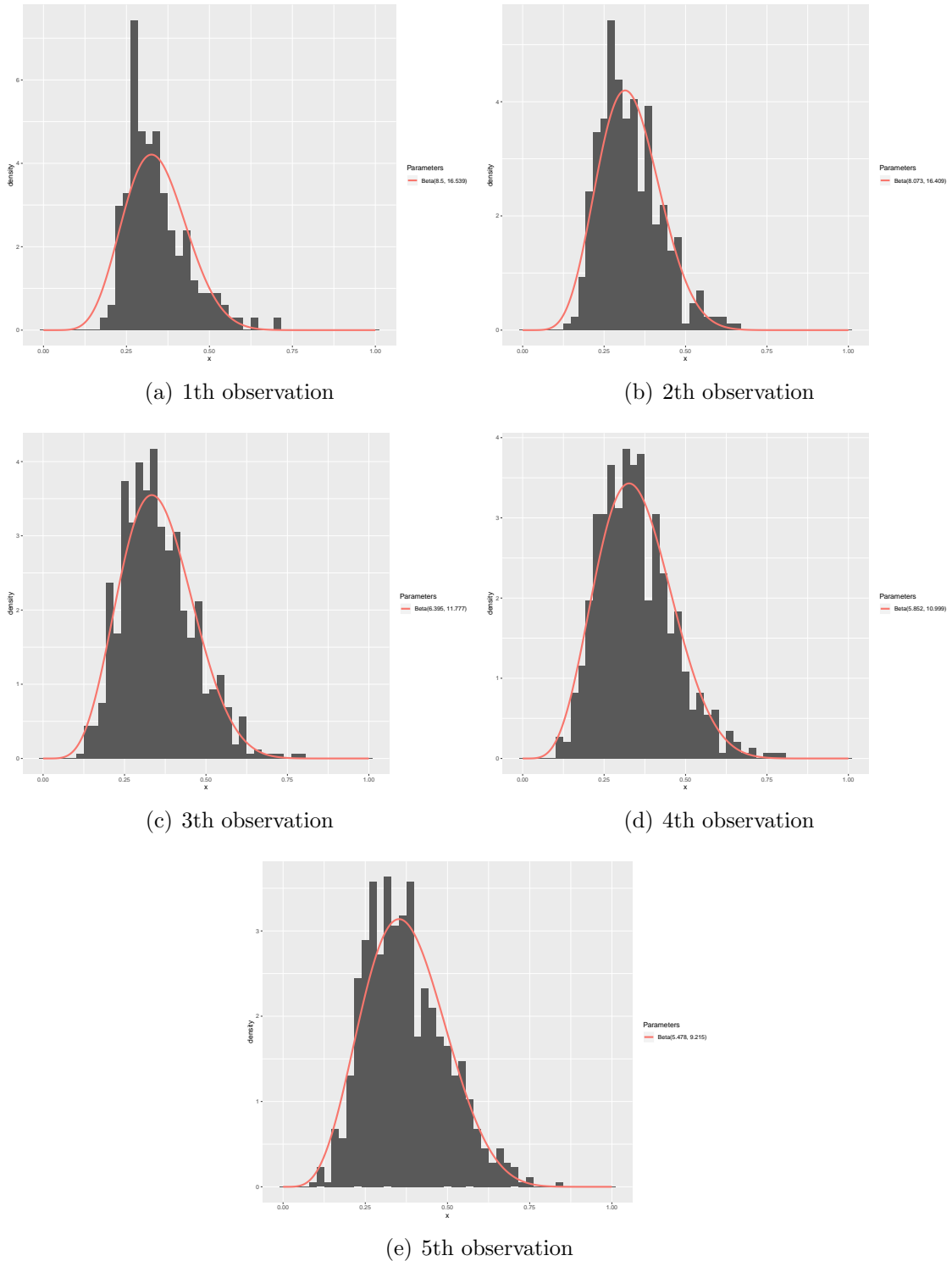


Figura 7: Histograms of the Geodesic Distances between random volume and the pixels of the sample extracted from Soybeans 231 most similar to random volume

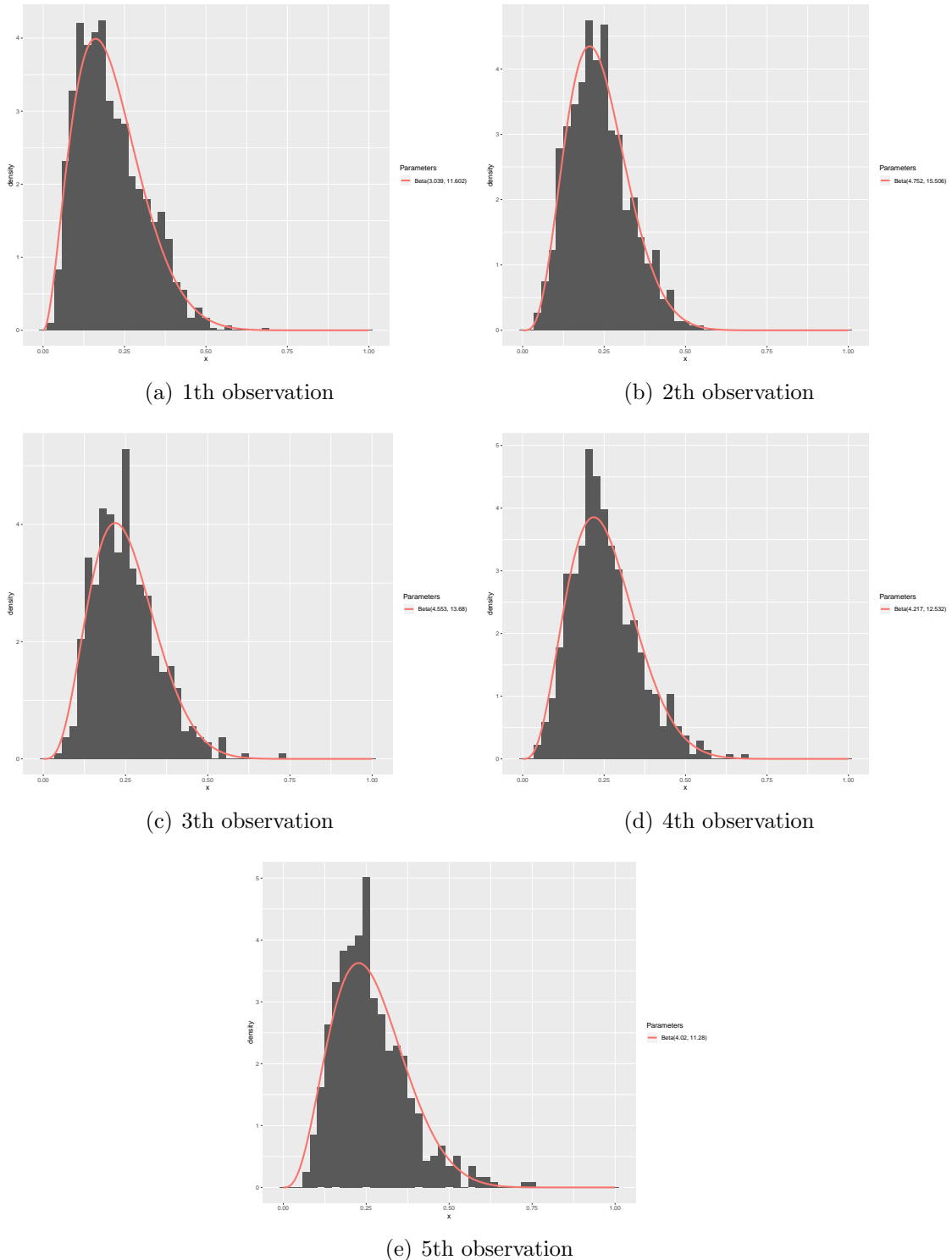


Figura 8: Histograms of the Geodesic Distances between trihedral and the pixels of the sample extracted from Soybeans 232 most similar to trihedral

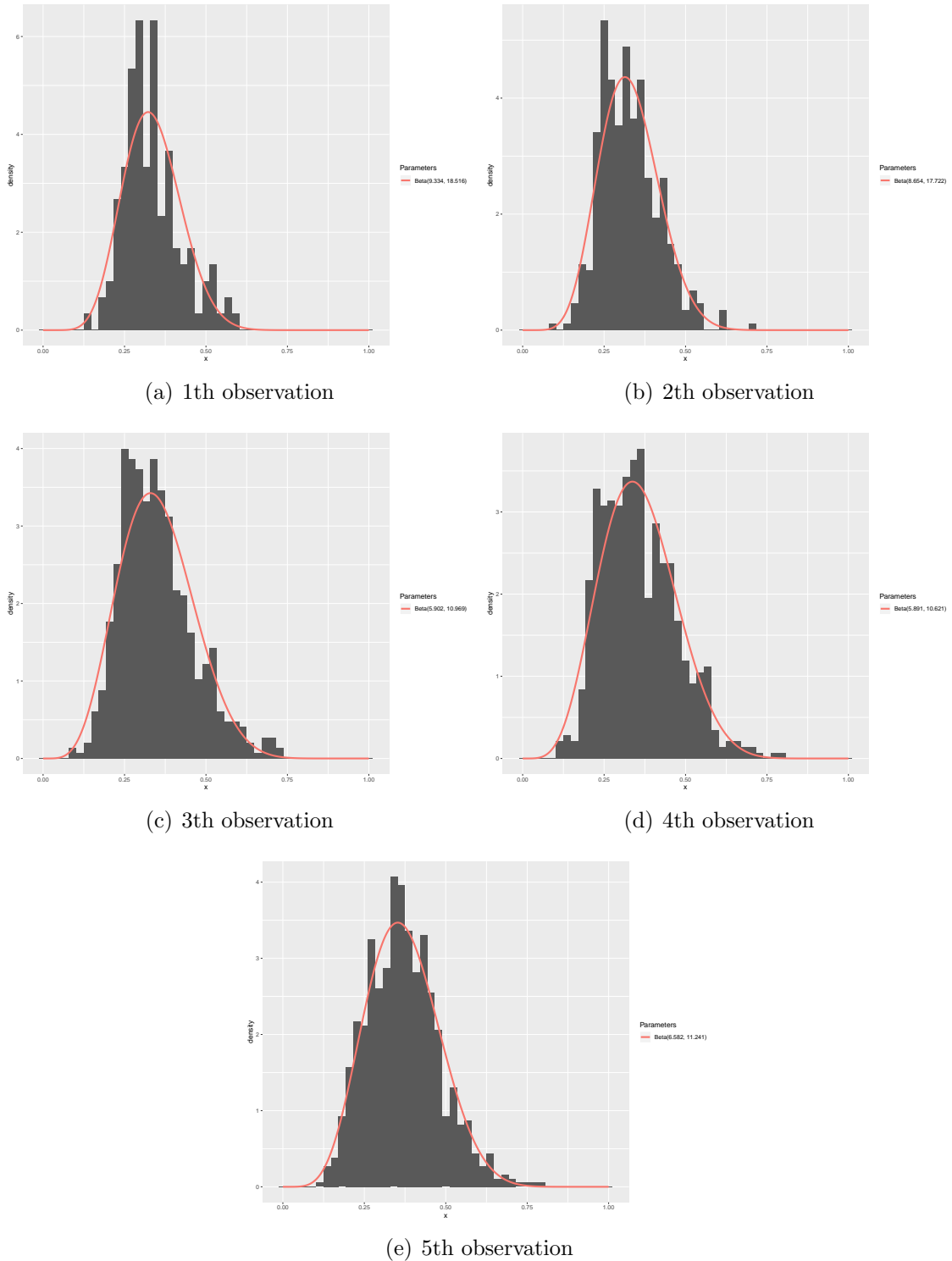
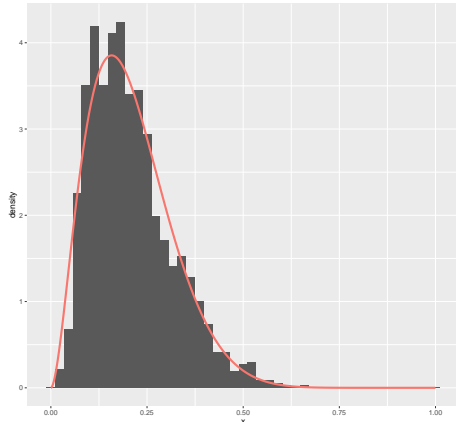
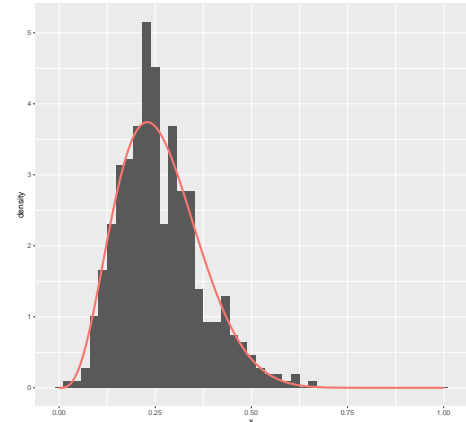


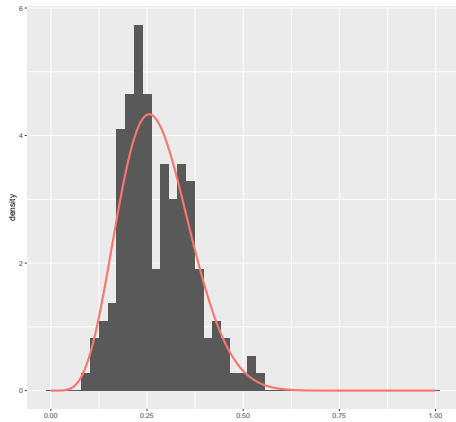
Figura 9: Histograms of the Geodesic Distances between random volume and the pixels of the sample extracted from Soybeans 232 most similar to random volume



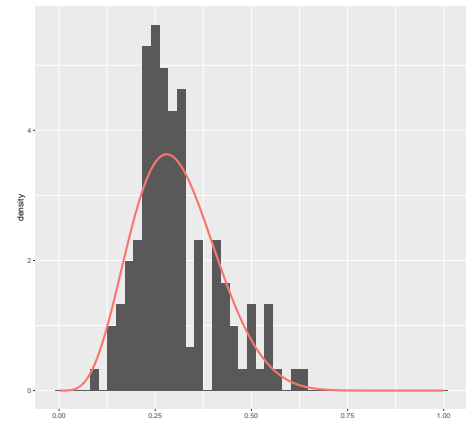
(a) 1th observation



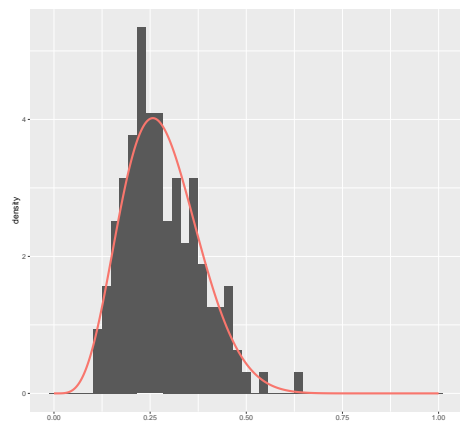
(b) 2th observation



(c) 3th observation



(d) 4th observation



(e) 5th observation

Figura 10: Histograms of the Geodesic Distances between trihedral and the pixels of the sample extracted from Wheat 104 most similar to trihedral

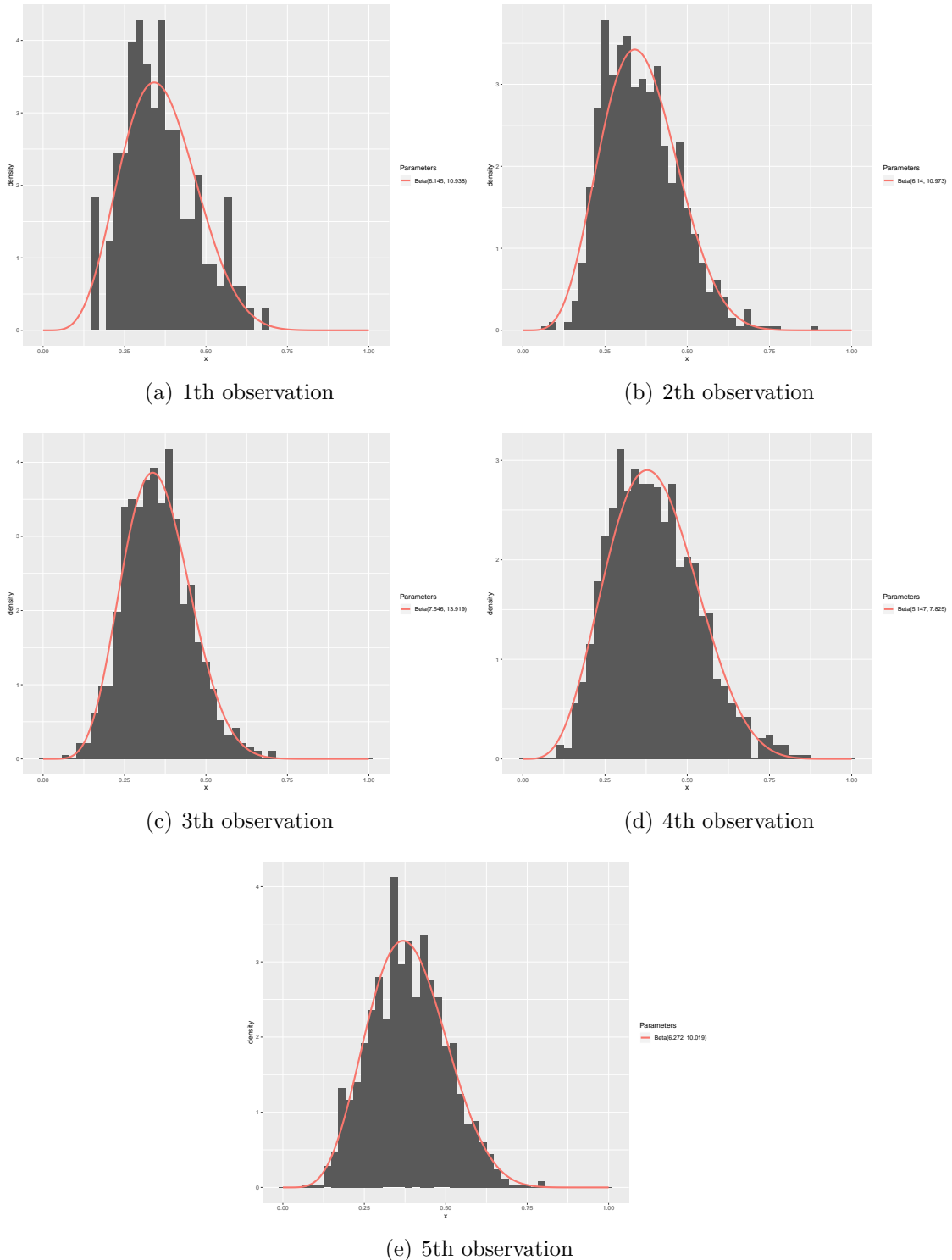
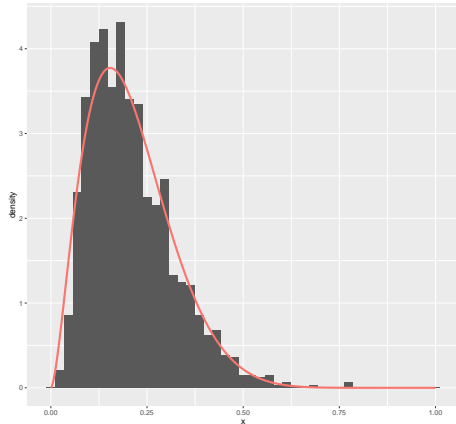
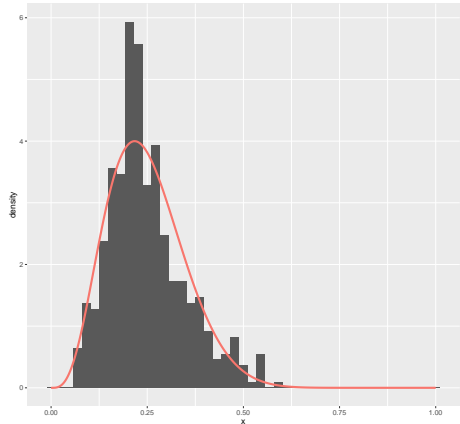


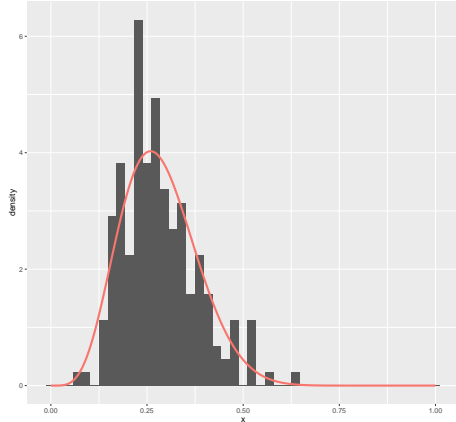
Figura 11: Histograms of the Geodesic Distances between random volume and the pixels of the sample extracted from Wheat 104 most similar to random volume



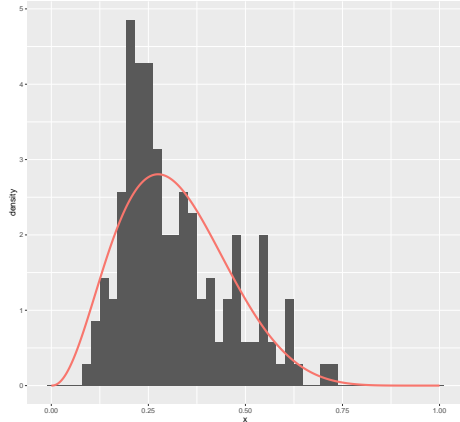
(a) 1th observation



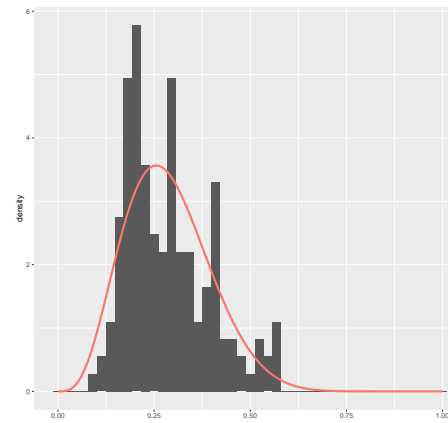
(b) 2th observation



(c) 3th observation



(d) 4th observation



(e) 5th observation

Figura 12: Histograms of the Geodesic Distances between trihedral and the pixels of the sample extracted from Wheat 105 most similar to trihedral

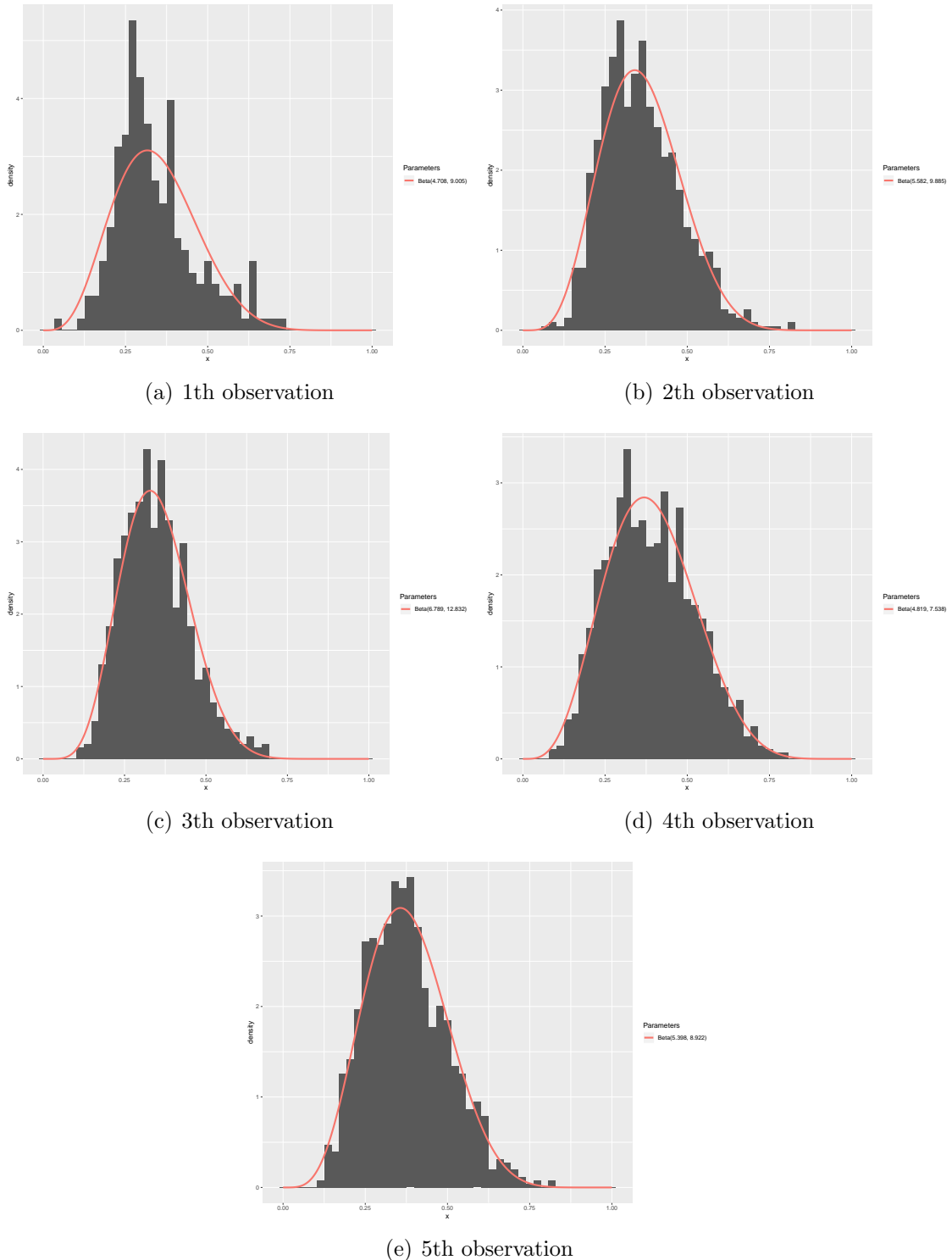
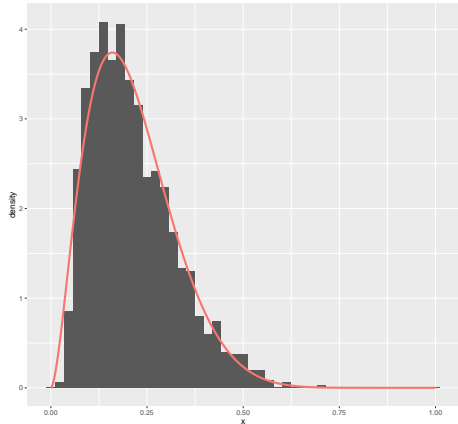
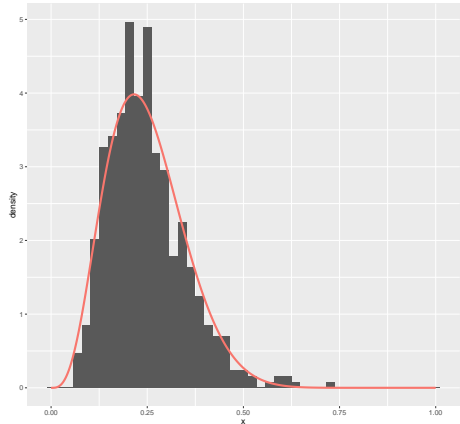


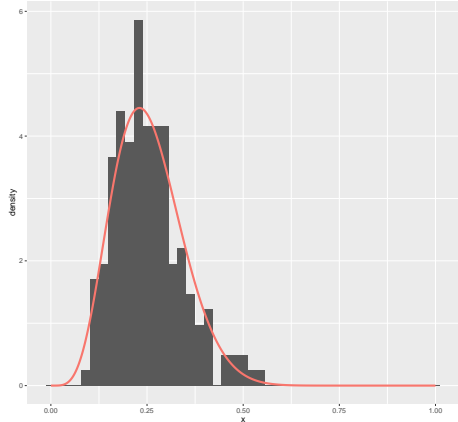
Figura 13: Histograms of the Geodesic Distances between random volume and the pixels of the sample extracted from Wheat 105 most similar to random volume



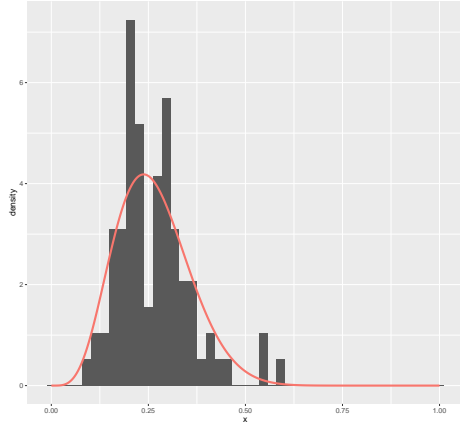
(a) 1th observation



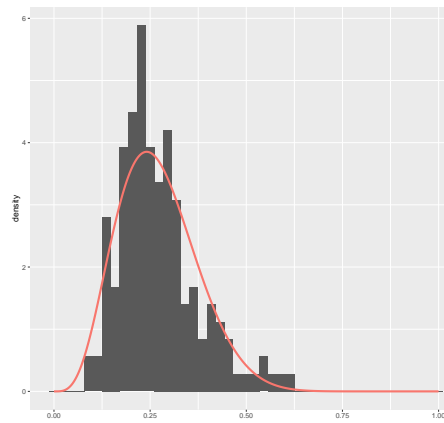
(b) 2th observation



(c) 3th observation



(d) 4th observation



(e) 5th observation

Figura 14: Histograms of the Geodesic Distances between trihedral and the pixels of the sample extracted from Wheat 255 most similar to trihedral

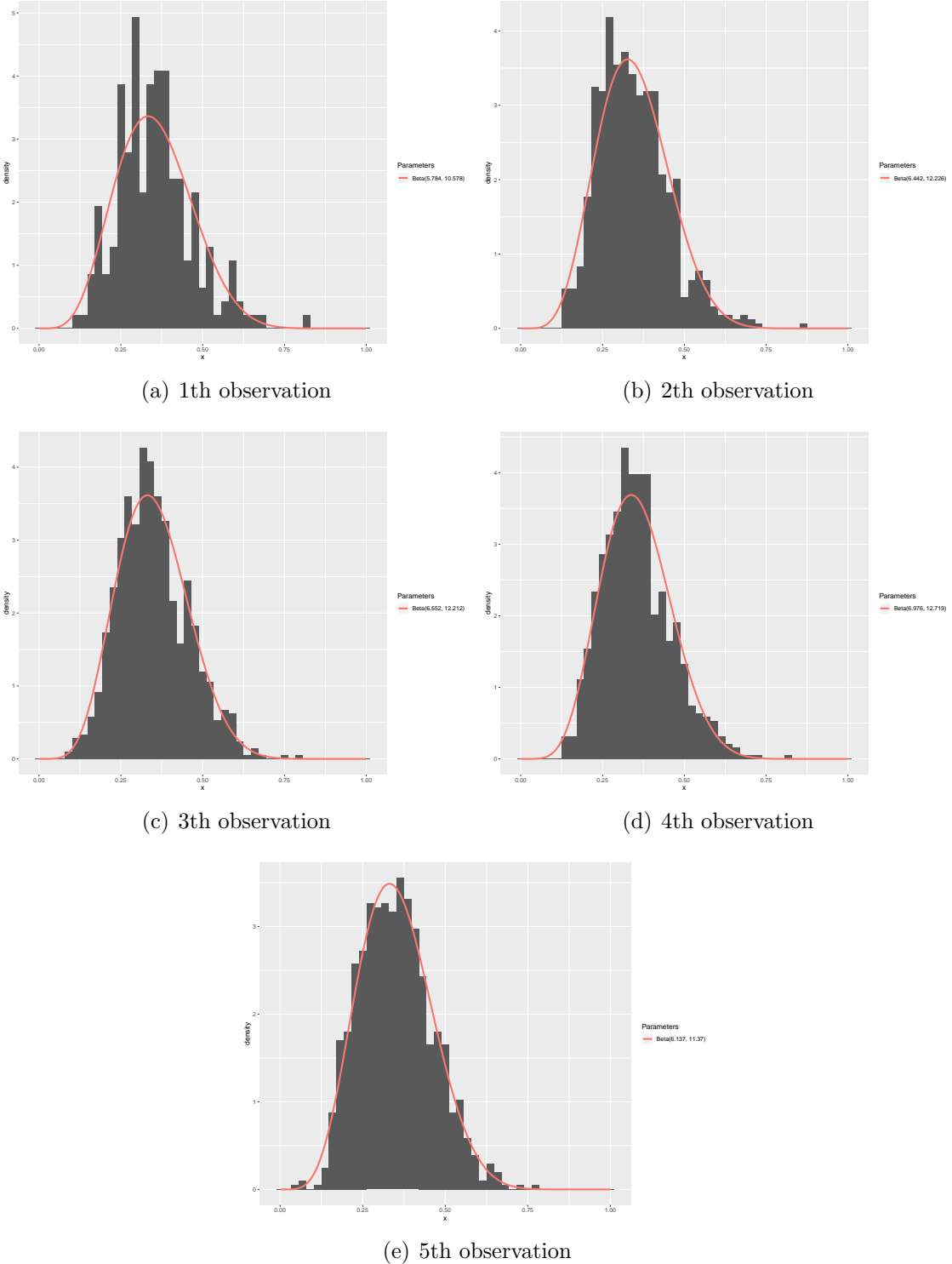


Figura 15: Histograms of the Geodesic Distances between random volume and the pixels of the sample extracted from Wheat 255 most similar to random volume

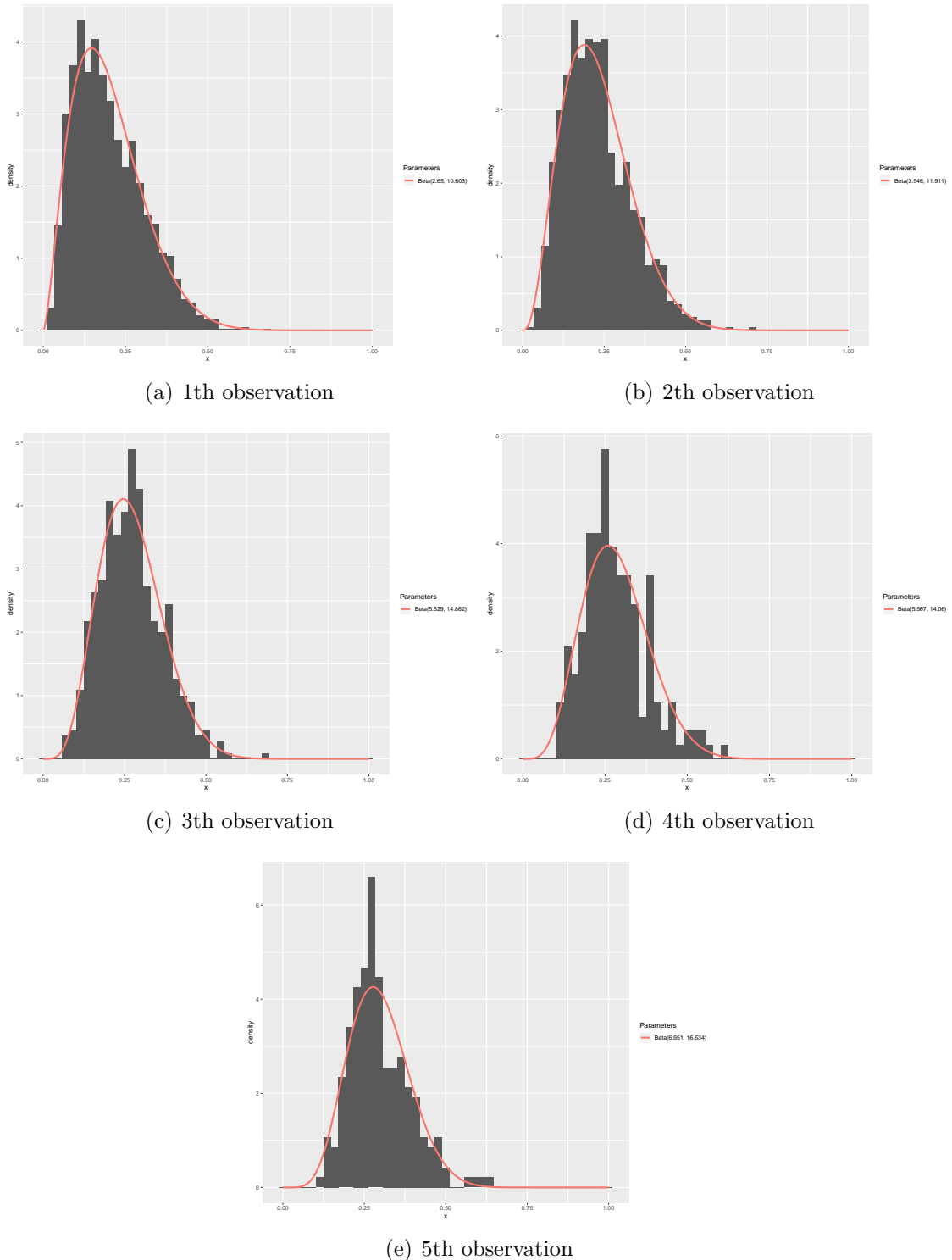


Figura 16: Histograms of the Geodesic Distances between trihedral and the pixels of the sample extracted from Canola 43 most similar to trihedral

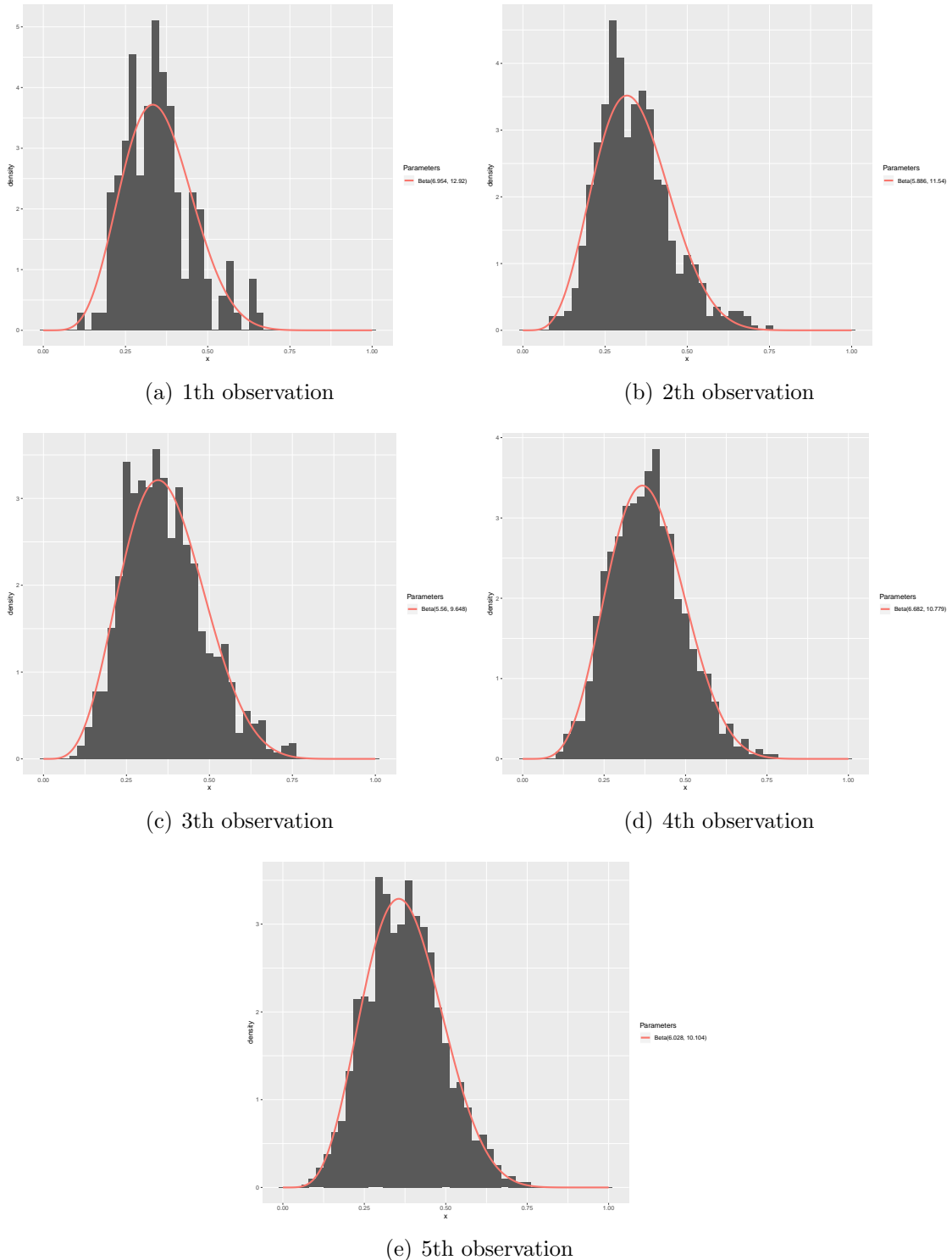
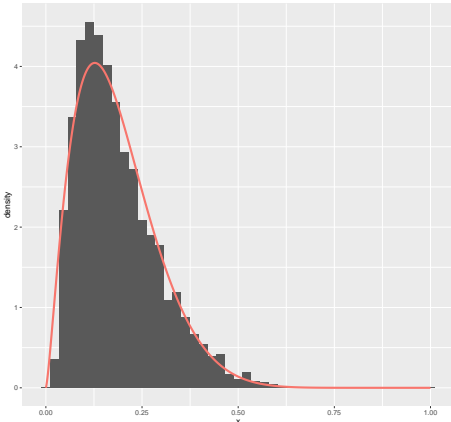
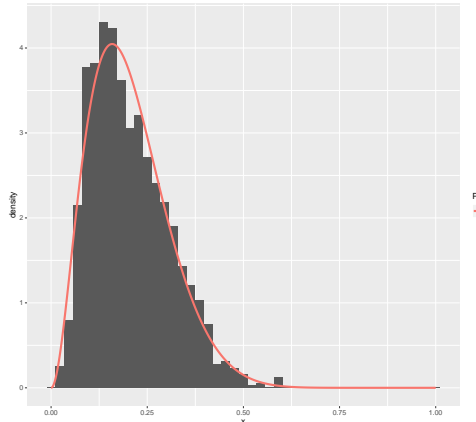


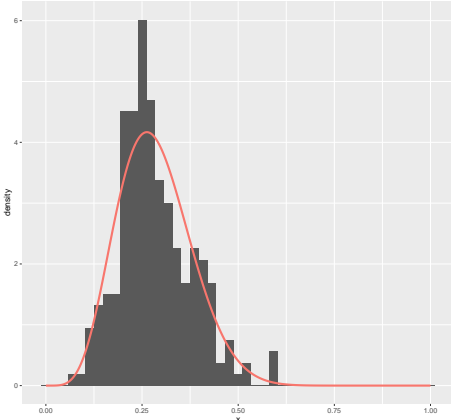
Figura 17: Histograms of the Geodesic Distances between random volume and the pixels of the sample extracted from Canola 43 most similar to random volume



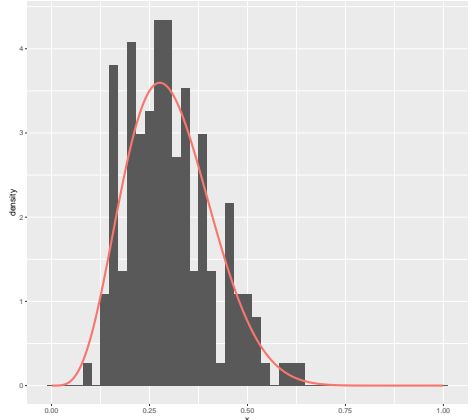
(a) 1th observation



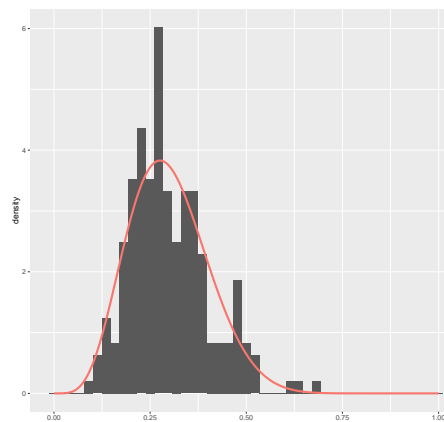
(b) 2th observation



(c) 3th observation



(d) 4th observation



(e) 5th observation

Figura 18: Histograms of the Geodesic Distances between trihedral and the pixels of the sample extracted from Canola 224 most similar to trihedral

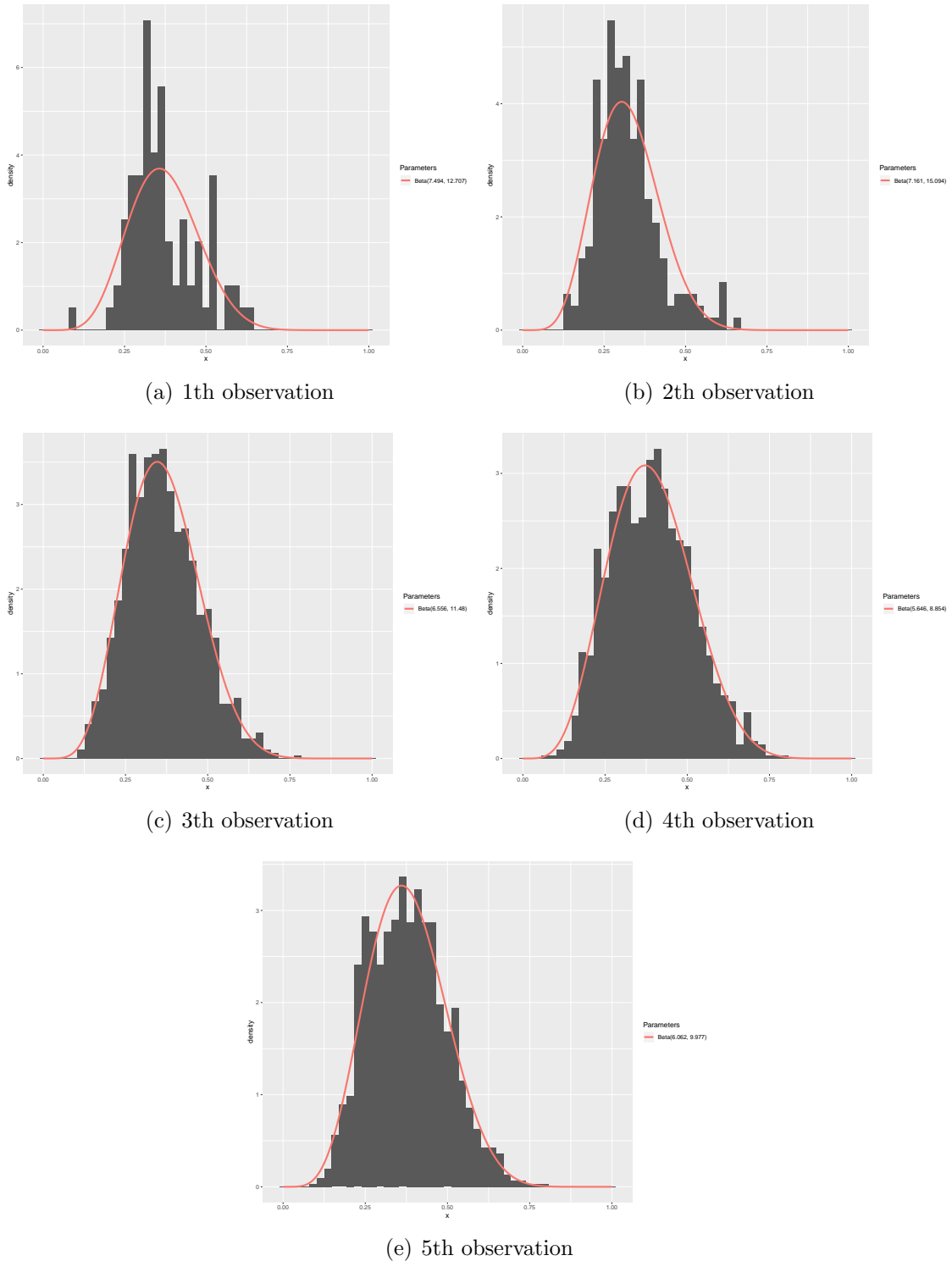


Figura 19: Histograms of the Geodesic Distances between random volume and the pixels of the sample extracted from Canola 224 most similar to random volume

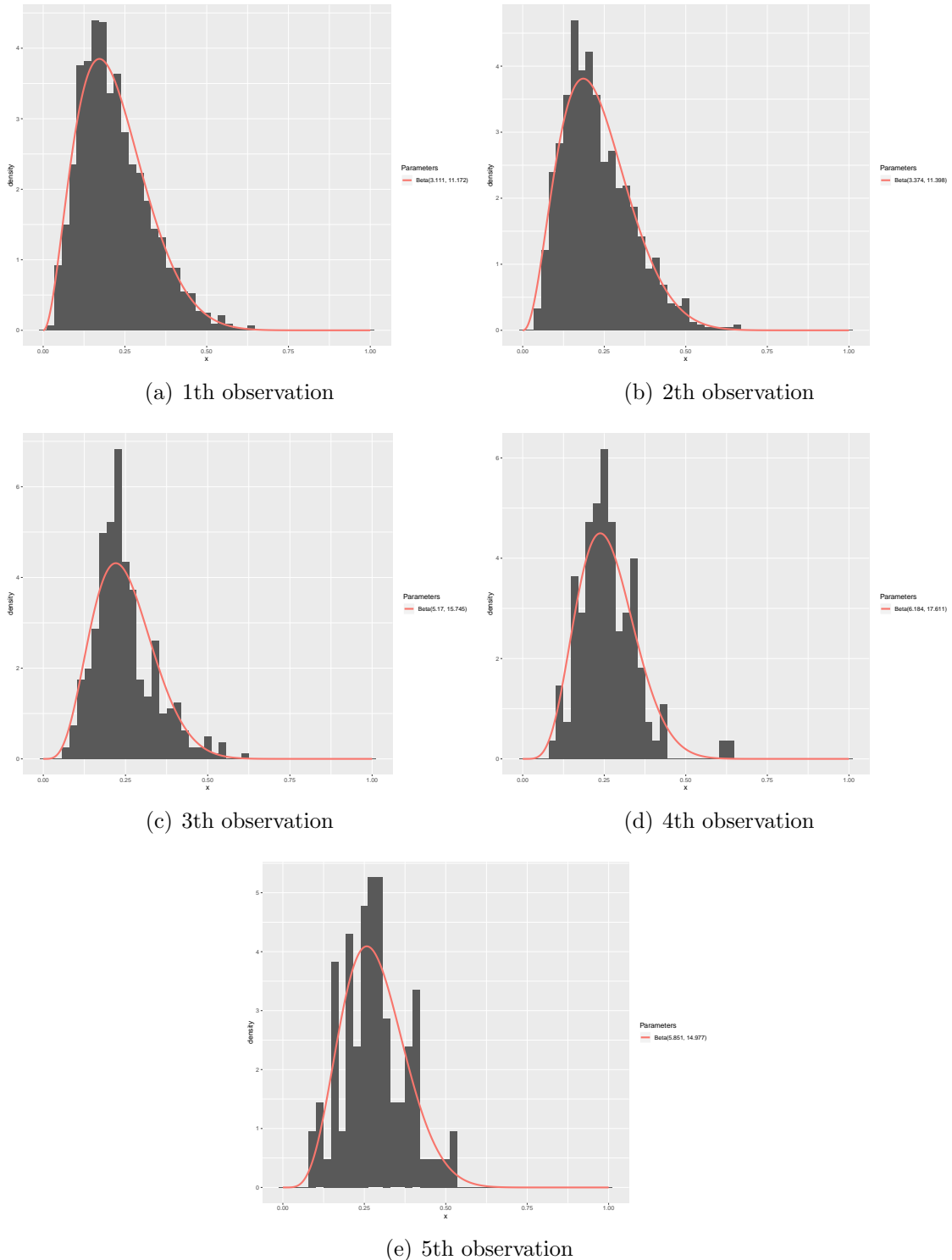


Figura 20: Histograms of the Geodesic Distances between trihedral and the pixels of the sample extracted from Oats 102 most similar to trihedral

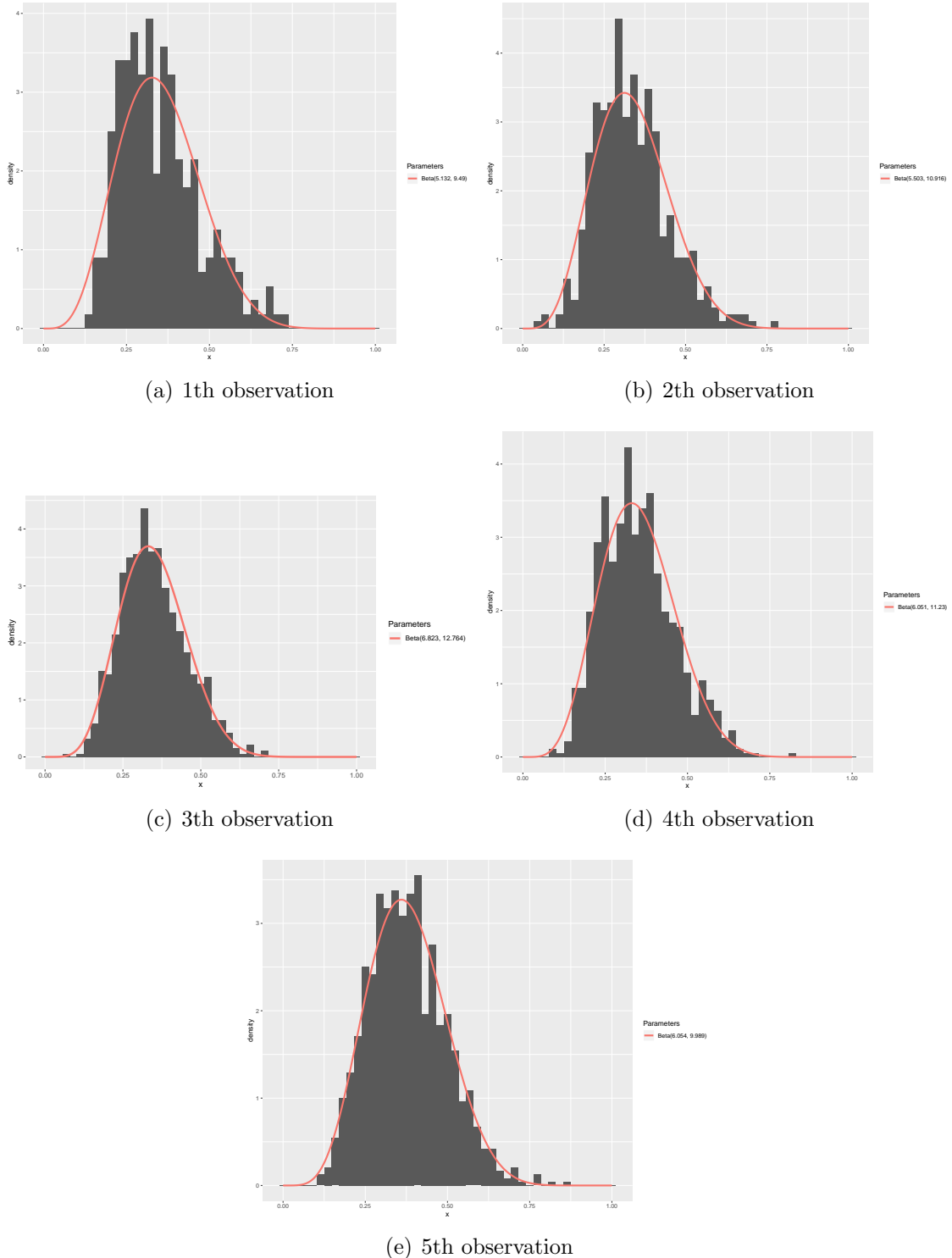
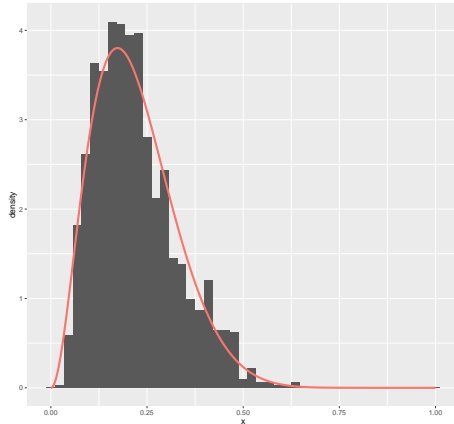
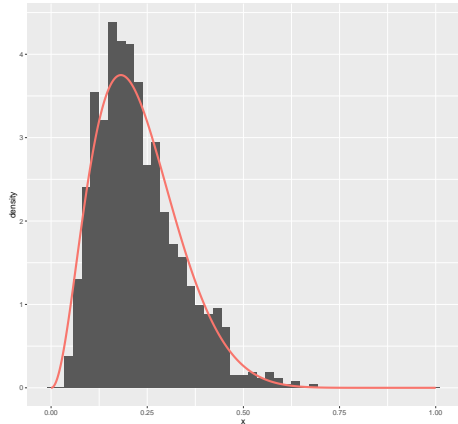


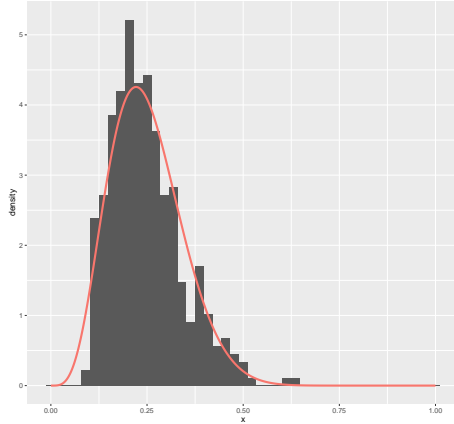
Figura 21: Histograms of the Geodesic Distances between random volume and the pixels of the sample extracted from Oats 102 most similar to random volume



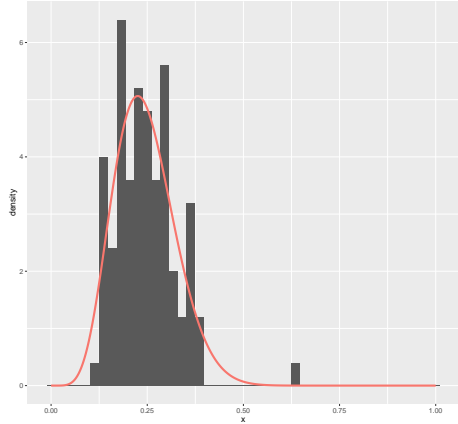
(a) 1th observation



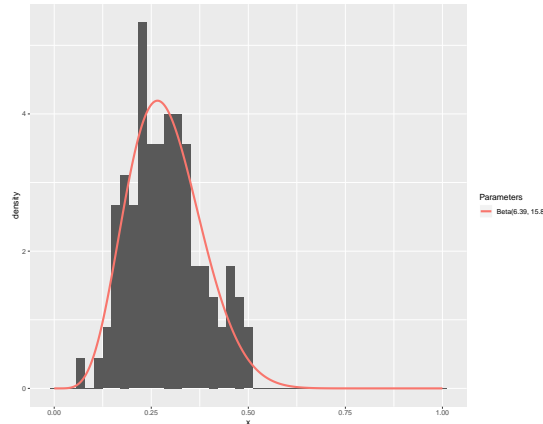
(b) 2th observation



(c) 3th observation



(d) 4th observation



(e) 5th observation

Figura 22: Histograms of the Geodesic Distances between trihedral and the pixels of the sample extracted from Oats 103 most similar to trihedral

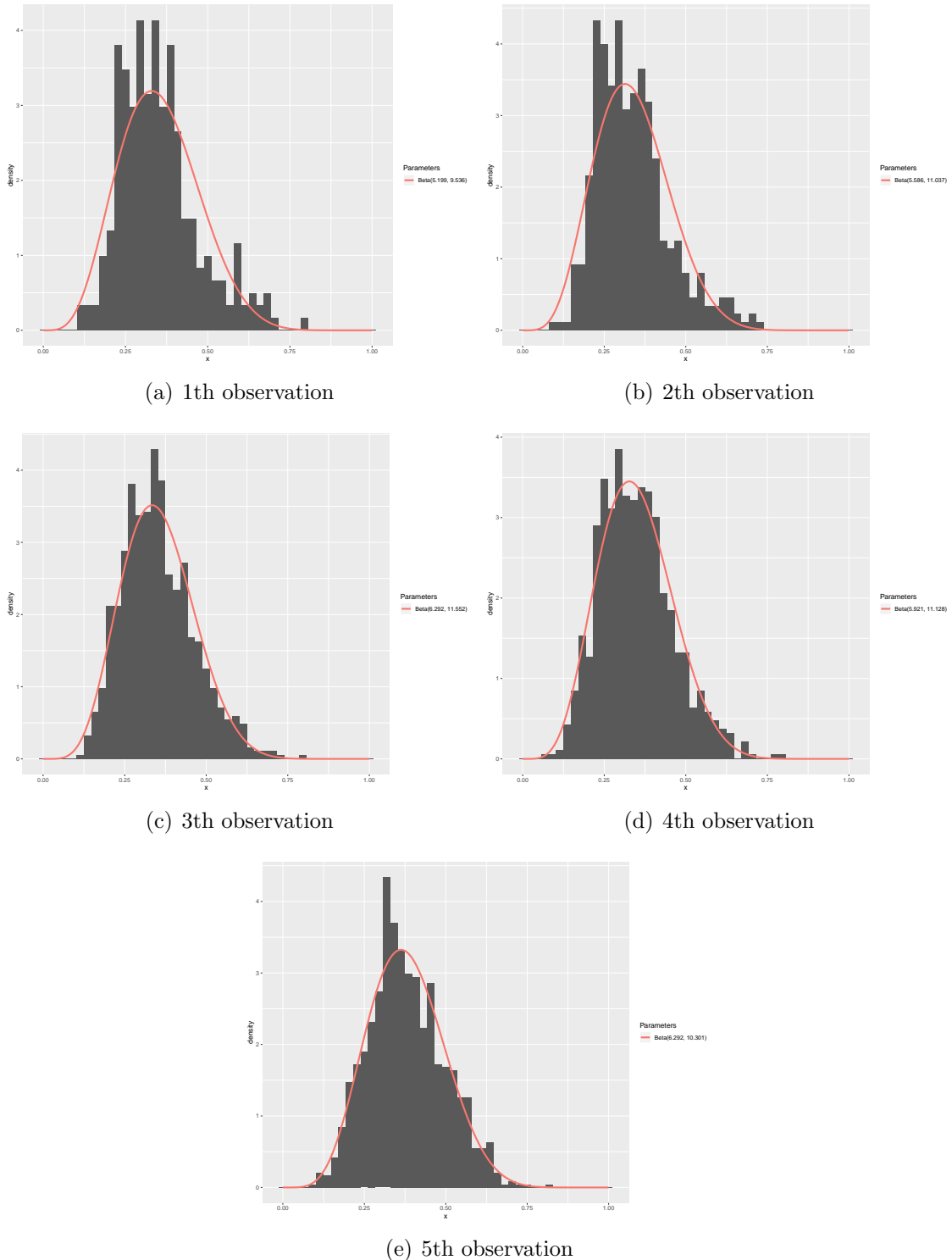


Figura 23: Histograms of the Geodesic Distances between random volume and the pixels of the sample extracted from Oats 103 most similar to random volume

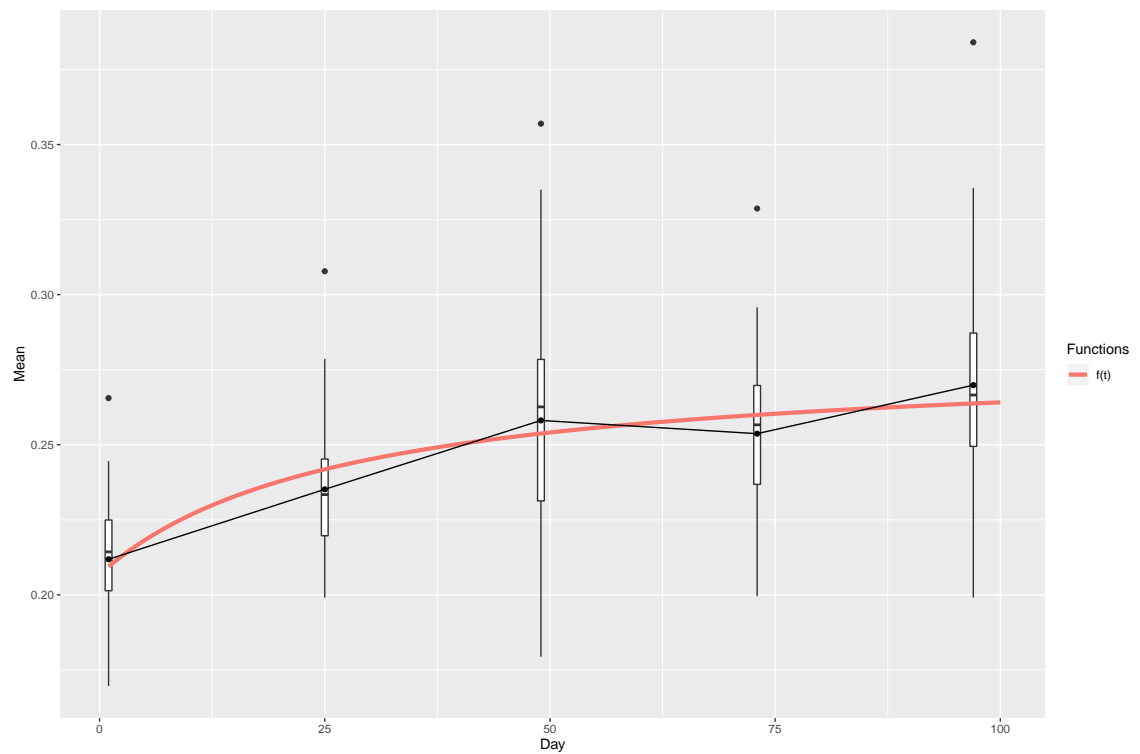


Figura 24: Mean of the distances between trihedral and samples extracted from Soybeans 231 over time